

High Contrast Probe Cleavage Detection

MICHAEL DUBROVSKY,^{1,2*} MORGAN BLEVINS², SVETLANA V. BORISKINA², DIEDRIK VERMEULEN¹

¹*Siphox Inc., 325 Vassar Street, Cambridge, MA 02139, USA*

²*Massachusetts Institute of Technology, 77 Massachusetts Avenue, Cambridge, MA 02139, USA*

*Corresponding author: Mike@siphox.com

Photonic biosensors that use optical resonances to amplify biological signals associated with the adsorption of low-index biological markers offer high-sensitivity detection capability, real-time readout, and scalable low-cost fabrication. However, they lack inherent target specificity and can be sensitive to temperature variations and other noise sources. In this letter, we introduce a concept of the High Contrast Probe Cleavage Detection (HCPCD) mechanism, which makes use of the dramatic optical signal amplification caused by cleavage of large numbers of high-contrast nanoparticle labels instead of the adsorption of low-index biological molecules. We illustrate numerically the HCPCD detection mechanism with an example of a silicon ring resonator as an optical transducer with gold and silicon nanoparticles as high-contrast labels. Simulations show that it is possible to detect a single cleavage-event by monitoring spectral shifts of micro-ring resonances. Furthermore, detection specificity and signal amplification can be achieved through the use of collateral nucleic acid cleavage caused by enzymes such as CAS12a and CAS13 after binding to a target DNA/RNA sequence.

In recent months, the need for a step-change in sensing technology to meet the challenges of the 21st century has been highlighted by the ongoing SARS-CoV-2 pandemic. Achieving high sensitivity in optical biosensors is a fundamentally difficult problem, as the sensitivity of any readout is limited by the small difference in optical properties between water (with refractive index of 1.33 in the visible range) and biomolecules (typically having refractive index of ~1.45). Target selectivity is even harder to achieve due to a comparable optical response induced by the adsorption of different biomolecules. However, biological machinery, such as the DNA primers and enzymes used for the polymerase chain reaction (PCR), routinely operates near single molecule concentrations and with very high selectivity [1]. In particular, clustered regularly interspaced short palindromic repeats (CRISPR)-associated systems serve as a defense mechanism against infection in prokaryotes, and are capable of site-specific cleavage of target (deoxy)ribonucleic acids (DNA/RNA) followed by non-specific cleavage of nucleic acids. Previous work in viral detection has shown that CRISPR CAS12a and CAS13

biological machinery can be harnessed to detect specific viral RNA or DNA strands [2,3], including recent efforts that have successfully shown SARS-CoV-2 detection [4,5]. CRISPR-based sensing techniques typically rely on measuring changes in the fluorescent response of probes (achieved via DNA/RNA oligo-probe cleavage to separate a quencher and a fluorophore), and thus require nucleic acid pre-amplification (e.g. PCR, LAMP) to reach attomolar sensitivity [6]. In principle, CRISPR-enabled single molecule detection is feasible, as a single CRISPR complex, activated by the hybridization of viral RNA/DNA to CRISPR RNA/DNA, produces thousands of non-specific collateral cleavages. However, fluorescent readout sets the lower limit for sensitivity in the fM range [2], and the nucleic acid pre-amplification process requires 1-3 hours of sample incubation, preventing real-time rapid screening.

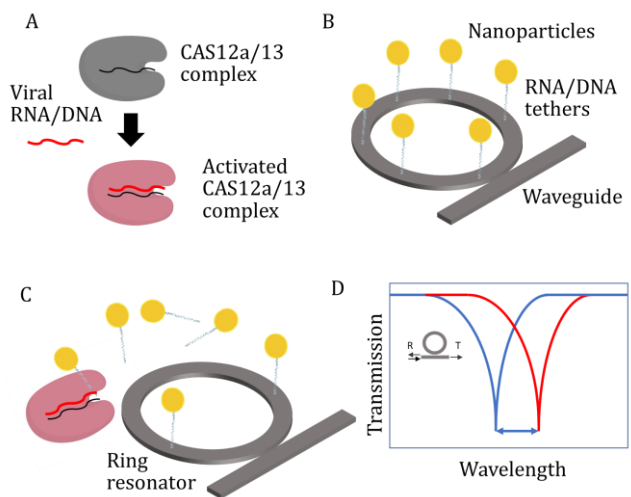


Fig. 1 Probe-Cleavage Detection combines CRISPR system specificity (a) with sensitive optical readout provided by optical micro-ring resonator (b) and amplification mechanism based on multiple nanoparticle probe cleavages triggered by every CRISPR complex activation (c). Probe cleavage results in a resonance red shift in the spectrum (d) of the ring.

Photonic biosensors that use micro-resonators as optical transducers offer a highly sensitive readout via monitoring

spectral shifts and intensity changes of narrow spectral resonances associated with excitation of resonator modes [7–9]. State-of-the-art chip-based photonic biosensors are capable of detecting antibodies when they bind to the antigen-functionalized resonator surfaces, as well as protein molecules and single viruses [10–14]. Detection sensitivity can be dramatically enhanced by using a combination of micro-resonators with high quality-factor photonic modes and metal nanoparticles supporting surface plasmon resonances [15–18], as well as using self-referenced sensor designs [19,20]. Molecular selectivity can be achieved via sensor surface functionalization (e.g. with antibody-specific antigens or target-complementary single strands of DNA and RNA). However, the sensor inability to distinguish between a perfect nucleotide match and a partial match and high noise levels due to non-specific adsorption events present significant practical challenges [21].

To achieve both, target selectivity and high sensitivity of detection, we propose to combine the detect-and-cleave biological mechanism of CRISPR systems with the robust and sensitive optical readout provided by a silicon photonic micro-ring resonator sensing platform (Fig. 1). A micro-resonator-based probe cleavage detection system needs to be functionalized with one or multiple nanoparticle probes, tethered onto a micro-resonator surface by DNA or RNA strands. If these probes are made of high-index metal or semiconductor material, the removal of even a single particle introduces a significant change in the resonator transmission spectrum, which can be sensed by the optical interrogation circuit. This is a key difference between the proposed HCPCD scheme and conventional approaches, which rely on the adsorption/capture of a low-index target molecule to generate a signal detected via the associated micro-resonator spectrum change. The probe removal can be achieved by designing the probe to be cleaved directly by the target analyte, or to be cleaved by a cleaving agent that has a specific detection mechanism for the target analyte. Once activated, the cleaving agent removes probes from the micro-resonator surface, leading to a detectable signal (Fig. 1). CRISPR Cas12 and Cas13 have been previously shown to cleave probes from a solid support in fluorescence-based viral diagnostic assay [22]. It should be noted that target molecules may be labeled with high contrast particles in the standard adsorption sensing architectures, nevertheless, this requires an additional binding step, which may significantly increase the sample processing time, and may reduce detection sensitivity and specificity.

We estimated numerically the optical effect of the removal of either a single or multiple high-contrast nanoparticles from a surface of a microring resonator, which is often used as an integrated optical transducer in on-chip (bio)-chemical sensing platforms. The Si microring supports high-quality-factor whispering-gallery (WG) modes, whose spectral positions and quality factors are sensitive to the changes in the ring nano-environment [23,24]. First, we used the Finite Difference Eigenmode solver (Lumerical MODE package) to calculate the spectral shift and the optical loss of a transverse-electric (TE) WG mode of a 20 micron diameter microring in a 1.55-micron band, which is caused by the cleavage of a tethered nanoparticle (Fig. 2). Figure 2a

illustrates the difference in the WG mode electric field profile in the microring cross-section before and after a single 10 nm radius gold (Au) nanoparticle is cleaved from its surface. Cleaving a particle off the resonator surface changes not only the local optical mode field profile but also the local effective index, leading to a change in spectral characteristics, including the resonant frequency and the optical loss (Fig. 2b). Since larger nanoparticles disturb the microring mode profile to a larger extent than smaller ones, cleavage of progressively larger Au nanoparticles generates larger resonance shifts. Our simulations predict blue shift of the WG mode resonant frequencies caused by the attachment of an Au nanoprobe, which is consistent with previous observations [25]. Accordingly, cleavage of an Au particle should result in a WG mode resonance redshift. Cleavage of dielectric nanoparticle probes can also be used as the detection mechanism. However, as shown in Fig. 2c for the case of a Si nanoparticle, the particle-induced mode redshift is an order of magnitude smaller than a blue shift caused by an Au probe of the same size, while the optical loss is negligible.

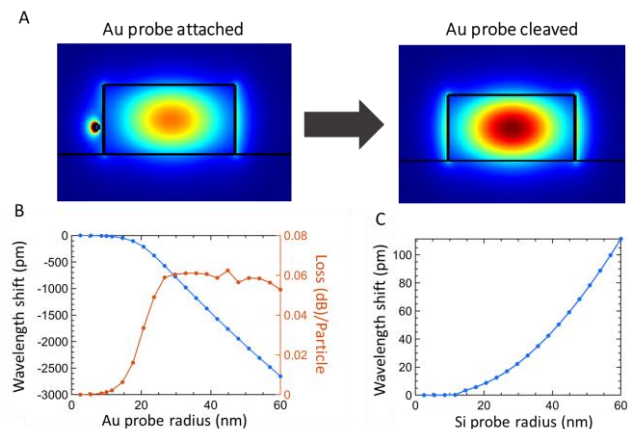


Fig. 2 (a) Electric field intensity profiles for the fundamental TE mode in a 500 nm wide and 220 nm thick strip silicon on insulator (SOI) waveguide in water before and after cleavage of a single 10-nm radius Au probe. (b-c) Spectral characteristics of a WG mode in a 20-micron diameter microring formed by looping the SOI waveguide, decorated by probes of varying size and material. (b) WG mode wavelength blue shift and optical loss caused by adding a single Au probe to the ring as a function of probe size. (c) WG mode wavelength redshift caused by a Si probe as a function of probe size (loss is negligible). In all the simulations, the probes are located 20 nm away from the ring surface.

To estimate the effect of the cleavage of multiple probes from a microring initially decorated by multiple Au nanoparticles, we performed three-dimensional finite difference time domain calculations of transmission spectra of a 20 micron diameter Si micro-ring resonator side-coupled to a bus Si waveguide via an 80nm gap (FDTD Lumerical package). The microring is initially decorated by fifty 10 nm radius Au probes and is excited by the fundamental TE guided mode of the bus waveguide. The signal transmitted through the waveguide exhibits narrow spectral dips at the wavelengths corresponding to WG mode resonances in the ring (Fig. 3a,b). Our calculations show that the resonant spectral features are progressively shifted to

longer wavelengths as more and more probes are removed from the microring surface, as would happen during cleavage in experimental conditions (Fig. 3a-c). Figure 3d shows a characteristic electric field distribution in a waveguide-coupled microring resonator.

We note that the wavelength shift predicted in our MODE simulations for a single 10 nm radius Au probe removal (10.68 pm) agrees qualitatively with the shift predicted by the 3D FDTD simulations (7.05 pm per particle on average). Importantly, this shift is about 5 times larger than the minimum shift that can be detected experimentally by using standard microring sensor architectures [9]. The practical limits of detection and time response in such a system may be determined by the diffusion rate of activated CRISPR complexes to the probe cleavage sites [26]. However, we have previously shown that WG mode resonators decorated by Au probes can capture biomolecules via optical trapping, reducing the detection time by two orders of magnitude beyond what can be expected due to diffusion [16], and similar enhancements have been observed in other resonator systems [27].

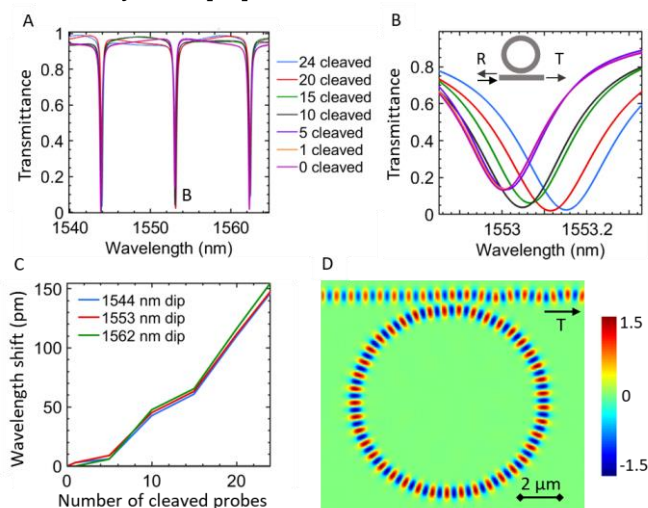


Fig. 3 (a) Transmission spectrum of a 20 micron diameter micro-ring resonator side-coupled to a one bus Si waveguide with the same parameters as in Fig. 2, initially decorated by 50 10 nm-radius Au probes located randomly around the ring circumference 20 nm away from its surface. The spectrum shifts as the number of attached probes is reduced to 26. (b) A magnified view of one of the WG mode resonances in (a). (c) The wavelength shifts for the three spectral dips in Fig. 3a as a function of the number of cleaved Au probes. (d) An electric field distribution in the system calculated at the wavelength of 1550 nm.

Silicon photonic sensors have been demonstrated to be very scalable via production in standard silicon photonic processes [28,29], allowing for low cost and multiplexing of multiple tests on the same analyte via microarray printing of functionalization chemistry onto individual rings. Detection sensitivity and specificity can also be increased by monitoring both TE and TM polarized modes supported by the microring [30]. Finally, the HCPCD approach is completely general, and can be combined with other optical transducers (e.g. surface plasmon resonance sensors or

Mach-Zehnder interferometers), as well as with electrical chip-based detection methods, and offers a pathway to highly sensitive real-time detection of biological molecules, viruses and other microorganisms. Any biosensing architectures based on analyte-induced enzymatic cleavage such as DNA-zyme biosensors [31] for sensing metal ions (as in water quality sensors) and Toehold Switch RNA sensors [32] are promising candidates for enhancement via HCPCD readout. More broadly, we hope the concept of communication between on-chip devices and biological systems via HCPCD can be generalized in the years to come as opto-biological nano-systems become more prevalent.

Acknowledgments. We thank Ke Du at RIT, John Connor at BU, Sharon Weiss at Vanderbilt University and Peter Nyugen at the Wyss Institute for helpful discussions as well as Mustafaa Hammood at UBC for assistance with the FDTD simulation setup. **Disclosures.** The authors declare no conflicts of interest.

References

- M. Kubista, J. M. Andrade, M. Bengtsson, A. Forootan, J. Jonák, K. Lind, R. Sindelka, R. Sjöback, B. Sjögreen, L. Strömbom, A. Ståhlberg, and N. Zoric, *Mol. Aspects Med.* **27**, 95 (2006).
- J. S. Gootenberg, O. O. Abudayyeh, J. W. Lee, P. Essletzbichler, A. J. Dy, J. Joung, V. Verdine, N. Donghia, N. M. Daringer, C. A. Freije, C. Myhrvold, R. P. Bhattacharyya, J. Livny, A. Regev, E. V. Koonin, D. T. Hung, P. C. Sabeti, J. J. Collins, and F. Zhang, *Science* **356**, 438 (2017).
- S.-Y. Li, Q.-X. Cheng, J.-M. Wang, X.-Y. Li, Z.-L. Zhang, S. Gao, R.-B. Cao, G.-P. Zhao, and J. Wang, *Cell Discov.* **4**, 20 (2018).
- J. P. Broughton, X. Deng, G. Yu, C. L. Fasching, V. Servellita, J. Singh, X. Miao, J. A. Streithorst, A. Granados, A. Sotomayor-Gonzalez, K. Zorn, A. Gopez, E. Hsu, W. Gu, S. Miller, C.-Y. Pan, H. Guevara, D. A. Wadford, J. S. Chen, and C. Y. Chiu, *Nat. Biotechnol.* (2020).
- F. Zhang, O. O. Abudayyeh, J. S. Gootenberg, *C. Sciences*, and L. Mathers, *Bioarchive* **1** (2020).
- Sherlock Biosciences, (2020).
- F. Vollmer and S. Arnold, *Nat. Meth.* **5**, 591 (2008).
- M. R. Foreman, J. Swaim, F. Vollmer, *Adv. Opt. Photonics* **7**, 168 (2015).
- E. Luan, H. Shoman, D. Ratner, K. Cheung, L. Chrostowski, *Sensors* **18**, 3519 (2018).
- M. R. Lee and P. M. Fauchet, *Opt. Express* **15**, 4530 (2007).
- F. Vollmer, S. Arnold, D. Keng, *Proc. Natl. Acad. Sci.* **105**, 20701 (2008).
- A. Yalçın, K. C. Popat, J. C. Aldridge, T. A. Desai, J. Hryniewicz, N. Chbouki, B. Little, O. King, V. Van, S. Chu, D. Gill, M. Anthes-Washburn, M. S. Ünlü, B. Goldberg, *IEEE J. Sel. Top. Quantum Electron.* (2006).
- C. Chao, W. Fung, L. J. Guo, *IEEE J. Sel. Top. Quantum Electron.* (2006).
- A. Nitkowski, A. Baeumner, M. Lipson, *Biomed. Opt. Express* (2011).
- M. A. Santiago-Cordoba, S. V. Boriskina, F. Vollmer, and M. C. Demirel, *Appl. Phys. Lett.* **99**, 073701 (2011).
- M. A. Santiago-Cordoba, M. Cetinkaya, S. V. Boriskina, F. Vollmer, and M. C. Demirel, *J. Biophotonics* **638**, 629 (2012).
- S. I. Shopova, R. Rajmangal, S. Holler, and S. Arnold, *Appl. Phys. Lett.* **98**, 243104 (2011).
- S. V. Boriskina, B. Reinhard, *Proc. Natl. Acad. Sci. USA.* **108**, 3147 (2011).
- S. V. Boriskina and L. Dal Negro, *Opt. Lett.* **35**, 2496 (2010).
- Y. Liu, Y. Li, M. Li, and J.-J. He, *Opt. Express* **25**, 972 (2017).
- B. N. Johnson and R. Mutharasan, *Analyst* **139**, 1576 (2014).
- K. N. Hass, M. Bao, Q. He, M. Park, P. Qin, and K. Du, *3*, 17 (2020).
- A. Yalçın, K. C. Popat, J. C. Aldridge, T. A. Desai, J. Hryniewicz, N. Chbouki, B. E. Little, O. King, V. Van, and S. Chu, *IEEE J. Sel. Top. Quantum Electron.* **12**, 148 (2006).
- A. Z. Subramanian, E. Ryckeboer, A. Dhakal, F. Peyskens, A. Malik, B. Kuyken, H. Zhao, S. Pathak, A. Ruocco, A. De Groot, P. Wuytens, D. Martens, F. Leo, W. Xie, U. D. Dave, M. Muneeb, P. Van Dorpe, J. Van Campenhout, W. Bogaerts, P. Bienstman, N. Le Thomas, D. Van Thourhout, Z. Hens, G. Roelkens, R. Baets, *Photon. Res.* **3**, B47 (2015).

25. A. Haddadpour and Y. Yi, *Biomed. Opt. Express* **1**, 378 (2010).
26. P. E. Sheehan and L. J. Whitman, *Nano Lett.* **5**, 803 (2005).
27. J. Su, A. F. G. Goldberg, and B. M. Stoltz, *Light Sci. Appl.* **5**, 2 (2016).
28. "Maverick™ Diagnostic System," <https://www.genalyte.com/clinical/>.
29. M. Iqbal, M. A. Gleeson, B. Spaugh, F. Tybor, W. G. Gunn, M. Hochberg, T. Baehr-jones, R. C. Bailey, and L. C. Gunn, *IEEE J. Sel. Top. Quantum Electron.* **16**, 654 (2010).
30. T. Claes, D. Vermeulen, P. De Heyn, K. De Vos, G. Roelkens, D. Van Thourhout, and P. Bienstman, in *XI Conf. Opt. Chem. Sens. and Biosens.* (2012), p. P-93 159.
31. R. J. Lake, Z. Yang, J. J. Zhang, Y. Lu, *Acc. Chem. Res.* **52**, 3275 (2019).
32. K. Pardee, A. A. Green, M. K. Takahashi, D. Braff, G. Lambert, J. W. Lee, T. Ferrante, D. Ma, N. Donghia, M. Fan, N. M. Daringer, I. Bosch, D. M. Dudley, D. H. O'Connor, L. Gehrke, J. J. Collins, *Cell* **165**, 1255 (2016).